

Auto-waveguide propagation and the collapse of spiral light beams in non-linear media

This article has been downloaded from IOPscience. Please scroll down to see the full text article.

1988 J. Phys. A: Math. Gen. 21 4381

(<http://iopscience.iop.org/0305-4470/21/23/020>)

View [the table of contents for this issue](#), or go to the [journal homepage](#) for more

Download details:

IP Address: 129.252.86.83

The article was downloaded on 31/05/2010 at 11:30

Please note that [terms and conditions apply](#).

Auto-waveguide propagation and the collapse of spiral light beams in non-linear media

V I Kruglov[†], V M Volkov[‡], R A Vlasov[†] and V V Driks[‡]

[†] Institute of Physics, BSSR Academy of Sciences, Leninsky prospekt 70, Minsk 220602, USSR

[‡] Institute of Mathematics, BSSR Academy of Sciences, Surganov str 11, Minsk 220602, USSR

Received 17 February 1988, in final form 8 June 1988

Abstract. The equation governing the propagation of spiral beams in a non-linear medium is analysed. It is shown that, taking into account the saturation effect, spiral beams have a tube-like structure with a periodicity along the axis of a non-linear autoguide. A critical power is found which it is necessary to exceed in order to give rise to the indicated autoguided regime of the beam propagation. Furthermore, in this work a strict self-similar solution is obtained of a non-linear Schrödinger-type equation that describes the collapse of spiral beams, and a new class of self-similar solutions is found for the case of spherical symmetry.

1. Introduction

It is well known that the non-linear refraction of rays in non-linear media results in self-focusing, self-trapping or defocusing of beams under appropriate conditions [1-6]. In particular, the autoguided propagation (self-trapping) of light beams takes place when the diffractive spread is compensated by the compression due to the non-linearity of dielectric permittivity. Many aspects of the theory of these phenomena are of interest, not only for optical applications. Indeed, there is a formal similarity between the equations of self-focusing theory and the Ginzburg-Landau equation, non-linear Schrödinger equation, etc, describing different phenomena. Hence, the results obtained in this domain acquire a certain generality.

The feasibility of forming new autoguided beams, called 'spiral' beams, with a non-zero topological charge has been predicted [7] and more recently confirmed [8, 9] by computational experiment. The data from the computer experiment show that these beams are stable. The beams are characterised by a spiral space-time phase structure and a ring-shaped radial distribution of the intensity (or the field modulus), i.e. their 3D view is tube-like (the intensity on the beam axis strictly equals zero). Note that the tube-like beams which are not autoguides have been considered elsewhere [10, 11].

In the present paper the space-time structure of spiral beams is studied on the basis of a numerical solution of the equation describing the behaviour of the spiral beams in a non-linear medium. It is shown that a spiral autoguided regime is feasible when a number of conditions, one of which is availability of saturation, are satisfied. In particular, a critical power is obtained, the excess of which is required to give rise to the above-mentioned regime. It is found that under no-saturation conditions a

collapse is possible, with the tube-like beam structure preserved. Contrary to the well known works on self-focusing, we have obtained an exact self-similar solution describing the collapse in the case of beams with an arbitrary topological charge. The results obtained hold true for 'ordinary' self-focusing when the topological charge equals zero. The self-similar solution found is consistent, to a high degree of accuracy, with the results of computer simulations.

2. An equation for the electric field of spiral beams in a non-linear medium

The propagation of a light beam in a non-linear medium is governed by the wave equation

$$\Delta \mathbf{E} - \frac{1}{c^2} \frac{\partial^2}{\partial t^2} (\varepsilon(\mathbf{E}_0) \mathbf{E}) = 0 \quad \mathbf{E} = \text{Re}\{\mathbf{E}_0 \exp[i(\omega t - Kz)]\} \quad (1)$$

where the dielectric permittivity may be written in the form

$$\varepsilon(\mathbf{E}_0) = \varepsilon_0 + \varepsilon_2(\mathbf{E}_0 \mathbf{E}_0^*) + \varepsilon_4(\mathbf{E}_0 \mathbf{E}_0^*)^2 + \dots \quad (2)$$

The peculiarity of the problem formulated in [7] is that the phase of the beam incident on the medium is dependent on the polar angle φ and may, in general, rotate at some angular rate Ω :

$$\mathbf{E}_0|_{z=0} = \mathbf{E}_1 \exp[i\phi(r, \varphi - \Omega t)]. \quad (3)$$

In the slowly varying amplitude approximation equation (1), which is written in the cylindrical coordinate system with regard to the terms of the second and fourth order in (2), takes the form

$$2iK \frac{\partial \mathbf{E}_0}{\partial z} = \frac{1}{r} \frac{\partial}{\partial r} \left(r \frac{\partial \mathbf{E}_0}{\partial r} \right) + \frac{1}{r^2} \frac{\partial^2 \mathbf{E}_0}{\partial \varphi^2} - 2i \frac{\omega}{c^2} \frac{\partial}{\partial t} (\varepsilon(\mathbf{E}_0) \mathbf{E}_0) + K_0^2 [\varepsilon_2(\mathbf{E}_0 \mathbf{E}_0^*) + \varepsilon_4(\mathbf{E}_0 \mathbf{E}_0^*)^2] \mathbf{E}_0 \quad (4)$$

where $K_0 = \omega/c$, $K = \sqrt{\varepsilon_0} K_0$. Taking into account equation (3) and the field periodicity relative to the spatial rotations, let us seek a solution of equation (4) as follows [7]:

$$\mathbf{E}_0(r, z, \varphi; t) = \mathbf{n} \mathcal{E}_0(r, z) \exp[-im(\varphi - \Omega t)] \quad m = \pm 1, \pm 2, \dots \quad (5)$$

Now, it is convenient to introduce a new function,

$$\mathcal{E}_0(r, z) = \psi(r, z) \exp(-imqz) \quad (6)$$

where $q = \sqrt{\varepsilon_0} \Omega/c$. Setting $q_0 = \Omega/c$ and taking into account the inequality $K_0 \gg |mq_0|$, with (5) and (6) substituted into (4), we obtain a non-linear stationary equation for $\psi(r, z)$:

$$2iK \frac{\partial}{\partial z} \psi = \left(\frac{\partial^2}{\partial r^2} + \frac{1}{r} \frac{\partial}{\partial r} - \frac{m^2}{r^2} \right) \psi + K_0^2 (\varepsilon_2 |\psi|^2 + \varepsilon_4 |\psi|^4) \psi. \quad (7)$$

It can be shown that a limited solution of equation (7) has asymptotics $|\psi| \sim r^{|m|}$ as $r \rightarrow 0$. For this reason, the boundary condition for equation (7), for $m = 0, \pm 2, \pm 3, \dots$, may be written as

$$\psi \Big|_{z=0} = \psi_0(r) \quad \frac{\partial \psi}{\partial r} \Big|_{r=0} = 0 \quad \lim_{r \rightarrow \infty} \psi(r, z) = 0. \quad (8)$$

Obviously, for $m = \pm 1$ the derivative $\partial\psi/\partial r$ has a singularity at $r = 0$, and therefore, in this case, another boundary condition should be used:

$$\psi|_{z=0} = \psi_0(r) \quad \psi|_{r=0} = 0 \quad \lim_{r \rightarrow \infty} \psi(r, z) = 0. \tag{9}$$

In this paper, the case considered is where $\varepsilon_2 > 0$, $\varepsilon_4 \leq 0$. Introducing dimensionless variables $r' = r/R_0$, $z' = z/2KR_0^2$, where R_0 is a characteristic radius of the beam, and a dimensionless complex function

$$u = u(r', z') = \sqrt{\varepsilon_2} R_0 K_0 \psi(r, z) \tag{10}$$

equation (7) is transformed to

$$i \frac{\partial u}{\partial z'} = \frac{1}{r'} \frac{\partial}{\partial r'} \left(r' \frac{\partial u}{\partial r'} \right) - \frac{m^2}{r'^2} u + (|u|^2 - \lambda |u|^4) u \tag{11}$$

where $\lambda = -\varepsilon_4/(\varepsilon_2 R_0 K_0)^2$.

Boundary conditions for the above equation may be expressed as follows:

$$u|_{z'=0} = u_0(r') \quad \left. \frac{\partial u}{\partial r'} \right|_{r'=0} = 0 \quad \lim_{r' \rightarrow \infty} u = 0 \quad m = 0, \pm 2, \pm 3, \dots \tag{12}$$

$$u|_{z'=0} = u_0(r') \quad u|_{r'=0} = 0 \quad \lim_{r' \rightarrow \infty} u = 0 \quad m = \pm 1. \tag{13}$$

The constants of motion I_1 and I_2 are important characteristics:

$$I_1 = \int_0^\infty |u|^2 r' dr' \tag{14}$$

$$I_2 = \int_0^\infty \left(\left| \frac{\partial u}{\partial r'} \right|^2 + \frac{m^2}{r'^2} |u|^2 - \frac{1}{2} |u|^4 + \frac{1}{3} \lambda |u|^6 \right) r' dr'. \tag{15}$$

It can be readily shown that

$$\frac{d}{dz} I_1 = 0 \quad \frac{d}{dz} I_2 = 0.$$

As will be shown below, the nature of the solution of equation (11) is mainly dependent on I_1 .

It should also be noted that the phase structure of the beam (5) has analogy with angular harmonics in the cavity [12]. Hence, the selected angular harmonics can serve as a source for forming the spiral autoguided beams considered here.

3. Results of computer simulations

The numerical solution of equation (11) with initial and boundary conditions (12) and (13) served as the basis for determining conditions under which the regime of autoguided spiral beam propagation is realised. The first necessary condition requires $\lambda > 0$, i.e. it takes account of the saturation effect. The second necessary condition is the inequality $\tilde{I}_1 > I_c$ where I_c is some critical parameter and \tilde{I}_1 is the energy localised in the beam. Note that $\tilde{I}_1 = I_1 - I_r$, where I_r is the energy part which is released by the beam. This implies that during the beam evolution in the z coordinate a part of the initial energy \tilde{I}_1 is localised along the z axis, and a part of the energy I_r is scattered

(radiated) in the radial direction. In the case of $I_1 < I_c$, a spread of the beam occurs. Note that I_c is dependent on m and the scattered energy I_r is dependent on the field profile on the medium boundary at $z=0$. It turned out that the ring-shaped field modulus distribution was necessary on the $z=0$ boundary to give rise to the spiral autoguided regime. In this case, the nearer the field distribution on the $z=0$ boundary to the autoguided solution, the smaller the energy I_r released by the beam. Since at a sufficiently large z one may always introduce some boundary radius \tilde{R} , separating the 'solitary' region of the beam from the scattered radiation, the energy \tilde{I}_1 localised in the beam may be defined as follows:

$$\tilde{I}_1 = \int_0^{\tilde{R}} |u(r', z')|^2 r' dr'. \quad (16)$$

In view of the above remark on the necessity of considering a ring-shaped field modulus distribution, the initial conditions for the function $u(r', z')$ at $z'=0$ were chosen as follows:

$$u(r', 0) = u_0(r') = g(r'^2/m^2) \exp[-(r'^2/2m^2)]. \quad (17)$$

As a result of the numerical solution of equation (11) with boundary conditions (12) and (13), it has been found that for $m = \pm 1$ the critical energy $I_c \approx 7.75$, and for $m = \pm 2, \pm 3, \dots$, ($\lambda \ll 1$), the energy I_c is approximately expressed by the formula $I_c \approx 7|m|$. It therefore became clear that the spiral autoguide always has a tube-like structure (a ring-shaped intensity distribution at any fixed z). This feature of the spiral autoguide has been theoretically predicted [7]. Another important result of the computer experiment is a discovered periodicity of the autoguided beam along the z axis [8, 9]. The character of autoguide oscillations is essentially dependent on the quantity $\Delta I_1 = \tilde{I}_1 - I_c$. With increasing ΔI_1 the frequency and amplitude of field oscillations increase as well. In the case of $\Delta I_1 \gg I_c$ a 'failure' arises when the periodicity is violated. Finally, the numerical calculations suggest the collapse regime at $\lambda = 0$, the solution being self-similar in this case:

$$|u(r', z')| = (z'_0 - z')^{-1/2} Q((z'_0 - z')^{-1/2} r'). \quad (18)$$

We draw attention to the fact that during collapse evolution, when $z' \rightarrow z'_0$ (z'_0 is the focusing point), $\max_{r'} |u(r', z')| \rightarrow \infty$ and the beam is compressed without limit but the tube-like structure remains (the field vanishes on the z axis).

The above conclusions on the spatial spiral beam structure are confirmed by the results of computer experiments presented in figures 1-3. Figure 1(a) illustrates the radial distribution of the field modulus at different values of z' . Figure 1(b) demonstrates the periodicity of the autoguided solution in z' . Within the oscillation period, the radial distribution of the amplitude modulus $|u(r', z')|$ has stages of spread and compression. In figure 1(a) plots 1-3 represent the radial distribution of the field amplitude modulus in the spread stage. The reverse order of the succession of the plots of figure 1(a) corresponds to the second part of the period, i.e. to the compression stage. The cases for other parameters of the problem ($m = 2, 3$) are shown in figures 2 and 3. Figure 4 represents the plot of the self-similar field amplitude distribution in the collapse regime ($\lambda = 0$).

We now discuss the role of the second motion constant in forming a spiral autoguide. By analogy with \tilde{I}_1 , we define the quantity \tilde{I}_2 as

$$\tilde{I}_2 = \int_0^{\tilde{R}} \left(\left| \frac{\partial u}{\partial r'} \right|^2 + \frac{m^2}{r'^2} |u|^2 - \frac{1}{2} |u|^4 + \frac{1}{3} \lambda |u|^6 \right) r' dr' \quad (19)$$

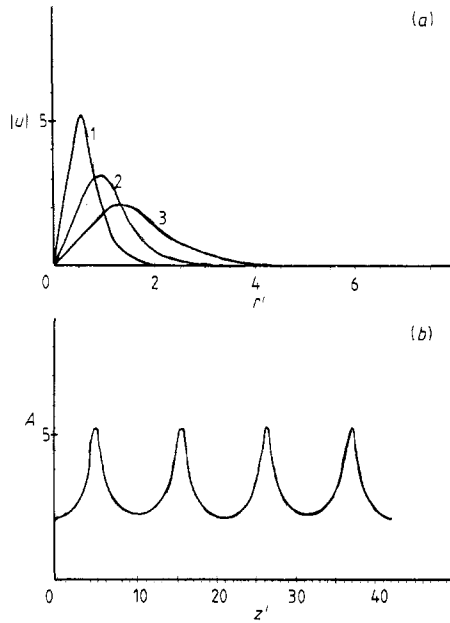


Figure 1. The structure of the spiral autoguided beam with initial field modulus distribution of the type (20) for $m = 1$, $g = 2\sqrt{2}$, $\lambda = \frac{1}{623}$. (a) The lateral distribution of $|u(r', z')|$ at different fixed values of z' . (b) z' dependence of maximum field amplitude $A(z') = \max_{r'} |u(r', z')|$

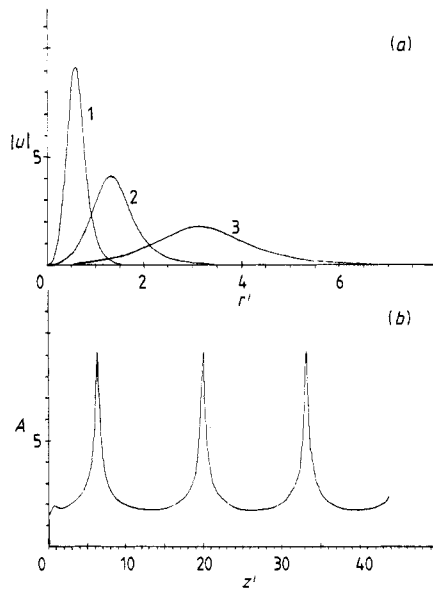


Figure 2. Same as figure 1 but $m = 2$.

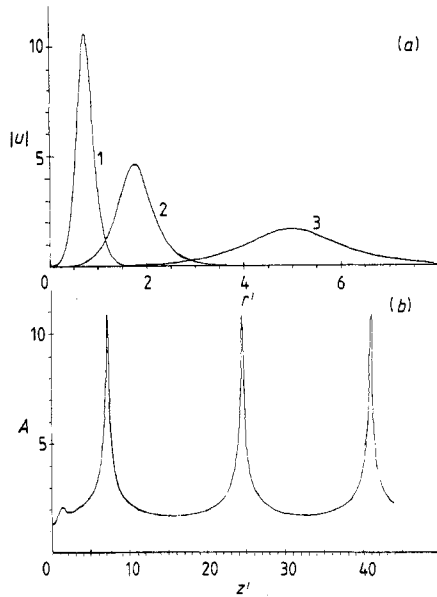


Figure 3. Same as figure 1 but $m = 3, g = 3$.

which is related to the localised part of the solution. Thus, the quantities \tilde{I}_1 and \tilde{I}_2 may be considered to be motion constants of the autoguide itself, the spatial spiral beam structure being largely dependent thereon. The computer experiment has shown that, in spite of the fact that $I_2 > 0$ corresponds to the initial distribution (17), after the release of energy the autoguide is characterised by the quantity $\tilde{I}_2 < 0$. Hence the motion constant I_1 plays a crucial role in forming the autoguided regime, since, as a result of scattering, the required condition $\tilde{I}_2 < 0$ is automatically provided at a sufficiently large z' . The restriction imposed on I_1 follows from the inequalities $\tilde{I}_1 > I_c, I_r > 0$ and has the form $I_1 = \tilde{I}_1 + I_r > I_c$.

The numerical results obtained allow the characteristic parameters of the spiral autoguide to be determined. In view of formulae (10) and (17) the field at the boundary of the medium ($z = 0$) may be expressed as

$$\psi(r, 0) = \frac{g}{\sqrt{\epsilon_2 R_0 K_0 m^2}} \left(\frac{r}{R_0}\right)^2 \exp\left[-\frac{1}{2m^2} \left(\frac{r}{R_0}\right)^2\right]. \tag{20}$$

Thus, although the parameter R_0 was not specified earlier, it follows from (20) that it yields a characteristic transverse dimension of the beam at the boundary of the medium. Hence, an arbitrarily chosen R_0 is associated with an arbitrary given initial condition for equation (7). The second independent parameter determining the field strength at the boundary is g . Further, for certainty, we take the following values: $g = \sqrt{8}, m = 2$ (figure 2), $\epsilon_2 = 10^{-20}$ CGSE and $K = 10^5 \text{ cm}^{-1}$, so that we choose the characteristic beam radius at $z = 0$ to be 0.1 cm in one case and 0.001 cm in the other. In consideration of the numerical results depicted in figure 2, the relations

$$r = R_0 r' \quad z = 2KR_0^2 z' \quad \psi(r, z) = u(r', z')/\sqrt{\epsilon_0 R_0 K_0}$$

are sufficient to find such parameters as the characteristic beam radii r_{\max} and r_{\min} corresponding to the maximum spread and maximum compression, respectively. Also,

these relations permit us to determine the period z_0 of autoguide oscillations and the maximum value of the field strength achieved at the points of maximum compression of the beam.

In the case under consideration, at $R_0 = 0.1$ cm, these parameters are of the order $r_{\max} \approx 0.3$ cm, $r_{\min} \approx 0.07$ cm, $z_0 \approx 3 \times 10^4$ cm, $\max_{r,z} \psi(r, z) \approx 10^7$ CGSE and, respectively, for $R_0 = 10^{-3}$ cm, $r_{\max} \approx 3 \times 10^{-3}$ cm, $r_{\min} \approx 7 \times 10^{-4}$ cm, $z_0 \approx 3$ cm, $\max_{r,z} \psi(r, z) \approx 10^9$ CGSE. Finally, we also evaluate the critical value of the energy integral which must be exceeded in order to realise the spiral autoguided regime. By definition

$$\mathcal{E} = \int_0^\infty |E_0|^2 r \, dr = \frac{1}{\epsilon_2 K_0^2} \int_0^\infty |u|^2 r' \, dr' = \frac{I_1}{\epsilon_2 K_0^2} \tag{21}$$

and therefore, for $m = 2$, $\epsilon_2 = 10^{-20}$ CGSE and $K_0 = 10^5$ cm⁻¹ we find $I_c \approx 7m / \epsilon_2 K_0^2 = 1.4 \times 10^{11}$ erg cm⁻¹.

Now, we discuss the appearance of oscillations in the spiral autoguide. The explanation appears to be associated with the fact that the last term in equation (10) may be ignored because λ is infinitesimal in the initial stage (small z). This leads to the evolution of the collapse. However, on compressing the beam and increasing the field strength, the non-linearity related to the saturation begins to take effect. Indeed, if the field strength is increased by an order of magnitude, the value of $\lambda |u|^4 u$ increases by a factor of 10^5 , and this term having the opposite sign begins to compete with the cubic non-linearity in (10). Further increases in z lead to the spread of the beam compressed in the initial stage of the evolution. As a result, the field intensity decreases, and the role of non-linearity of the fifth order of magnitude once again becomes negligible. The collapse stage then resumes. The oscillatory process is thus self-maintained.

4. Two-dimensional collapse of spiral beams

In the theory of non-linear wave processes the collapse plays the same fundamental role as solitons. There are several widely known examples of wave collapses as singularity formations for finite time. Some phenomena concerned are: the formation of discontinuities in gas dynamics, self-focusing of light beams in non-linear media, the collapse of plasma waves, etc. In particular, the problem of collapse was investigated [13–19]. Unlike the soliton regime, under collapse conditions the balance between dispersional (or diffractive) wave spread and the non-linear compression process is disturbed, so that the latter dominates. From the data of the computer experiment, there are two regimes in the case of spiral beam propagation described by equation (7): (a) either the spread of the beam for $I_1 < I_c$ or (b) the formation of the pulsing autoguide, the necessary condition for which is $I_1 > I_c$. However, this occurs at $\epsilon_4 < 0$ only. In the case of $\epsilon_4 = 0$ there takes place either the collapse when $I_1 > I'_c$, or spread when $I_1 < I'_c$. Note that for $\lambda \ll 1$ we have $I_c \approx I'_c$. Thus, the collapse of spiral beams is governed by the equation

$$2iK \frac{\partial}{\partial z} \psi = \left(\frac{\partial^2}{\partial r^2} + \frac{1}{r} \frac{\partial}{\partial r} - \frac{m^2}{r^2} \right) \psi + G |\psi|^2 \psi \tag{22}$$

where $G = \epsilon_2 K_0^2$. For $m = 0$ this equation describes ordinary self-focusing.

Let us represent the function $\psi(r, z)$ as

$$\psi(r, z) = A(r, z) \exp(i\phi(r, z)). \tag{23}$$

Equation (22) then reduces to a system of two equations for the real functions $A(r, z)$ and $\phi(r, z)$:

$$2KA_z = 2\phi_r A_r + [\phi_{rr} + (1/r)\phi_r]A \tag{24}$$

$$(\phi_r^2 - 2K\phi_z)A = A_{rr} + (1/r)A_r - (m^2/r^2)A + GA^3. \tag{25}$$

Let the solution sought be of the form

$$A(r, z) = g(z)F(rf(z)) = g(z)F(R) \quad R = rf(z) \tag{26}$$

so that equation (24) takes the form

$$2Kg'(z)F(R) + 2Krg(z)f'(z)F'(R) = 2\phi_r g(z)f(z)F'(R) + [\phi_{rr} + (1/r)\phi_r]g(z)F(R). \tag{27}$$

Our primary assumption is that the members containing $F(R)$ and $F'(R)$ are essentially different, and therefore they should be separately equated to each other in the left- and right-hand side of equation (27). Thus, we arrive at the system of equations

$$Krf'(z) - \phi_r f(z) = 0 \tag{28}$$

$$2Kg'(z) - [\phi_{rr} + (1/r)\phi_r]g(z) = 0 \tag{29}$$

which is a particular case of (27). It follows from equation (28) that

$$(1/Kr)\phi_r = c(z) \quad \phi(r, z) = \frac{1}{2}Kc(z)r^2 + \varphi(z) \tag{30}$$

where $c(z)$ and $\varphi(z)$ are some unknown functions.

Substituting (30) into (28) and (29) we find

$$f'(z) - c(z)f(z) = 0 \quad g'(z) - c(z)g(z) = 0 \tag{31}$$

whence $f(z) = \lambda g(z)$. Without loss of generality, one may set $\lambda = 1$ and hence $f(z) = g(z)$. Substituting the expression for phase (30) into (25) and taking account of $f(z) = g(z)$ and $R = rf(z)$, we come to the equation which is basic for the subsequent analysis:

$$K^2(c^2(z) - c'(z))f^{-4}(z)R^2F(R) - 2K\varphi'(z)f^{-2}(z)F(R) = F''(R) + (1/R)F'(R) - (m^2/R^2)F(R) + GF^3(R). \tag{32}$$

Let us consider two different cases which are determined by equation (32). In the first case we set

$$c'(z) - c^2(z) = 0 \tag{33}$$

$$2K\varphi'(z) + \zeta^2 f^2(z) = 0 \tag{34}$$

and then from equations (31) and (33) we find

$$c(z) = \frac{1}{z_0 - z} \quad f(z) = \frac{b}{z_0 - z}. \tag{35}$$

Here z_0 and b are integration constants. Now, solving equation (34), we determine $\varphi(z)$:

$$\varphi(z) = \phi_0 - \frac{b^2 \zeta^2}{2K(z_0 - z)} \quad \phi_0 = \text{constant}. \tag{36}$$

In view of (26), (30), (32) (35) and (36), we arrive at the first self-similar case:

$$A(r, z) = \frac{b}{(z_0 - z)} F\left(\frac{br}{z_0 - z}\right) \tag{37}$$

$$\phi(r, z) = \phi_0 + \frac{K^2 r^2 - b^2 \zeta^2}{2K(z_0 - z)} \tag{38}$$

where $F(R)$ satisfies the following equation and boundary conditions:

$$F''(R) + (1/R)F'(R) - [(m^2/R^2) + \zeta^2]F(R) + GF^3(R) = 0 \tag{39}$$

$$\lim_{R \rightarrow 0} F'(R) = 0 \quad \lim_{R \rightarrow \infty} F(R) = 0 \quad F(R) \geq 0. \tag{40a}$$

Here $m = 0, \pm 2, \pm 3, \dots$. Since the function $F(R)$ has asymptotics $F(R) \sim R^{|m|}$ as $R \rightarrow 0$, the required boundary condition for equation (39) at $m = \pm 1$ is

$$\lim_{R \rightarrow 0} F(R) = 0 \quad \lim_{R \rightarrow \infty} F(R) = 0 \quad F(R) \geq 0. \tag{40b}$$

The case where $b > 0, z < z_0$ corresponds to the collapse. Another (damped) solution is obtained if $b < 0, z > z_0$.

Now let us proceed to the consideration of the second case. From the analysis of equation (32) it follows that the conditions to be satisfied are

$$c'(z) - c^2(z) = (1/4b^2)f^4(z) \tag{41}$$

$$2K\varphi'(z) + \zeta^2 f^2(z) = 0. \tag{42}$$

The solution of the system of equations (31) and (41) is

$$c(z) = \frac{1}{2(z_0 - z)} \quad f(z) = \left(\frac{b}{z_0 - z}\right)^{1/2} \tag{43}$$

where z_0 and b are integration constants. Solving (42), taking account of (43), we determine $\varphi(z)$:

$$\varphi(z) = \phi_0 + \frac{b\zeta^2}{2K} \ln \left| \frac{z_0 - z}{b} \right| \quad \phi_0 = \text{constant}. \tag{44}$$

Therefore, taking account of (26), (30), (32), (43) and (44) we arrive at the second self-similar case:

$$A(r, z) = \left(\frac{b}{z_0 - z}\right)^{1/2} F\left(\left(\frac{b}{z_0 - z}\right)^{1/2} r\right) \tag{45}$$

$$\phi(r, z) = \phi_0 + \frac{Kr^2}{4(z_0 - z)} + \frac{b\zeta^2}{2K} \ln \left| \frac{z_0 - z}{b} \right|. \tag{46}$$

Here, in accordance with (32), the function $F(R)$ satisfies the following equation and boundary conditions for $m = 0, \pm 2, \pm 3, \dots$:

$$F''(R) + (1/R)F'(R) - [(m^2/R^2) + \zeta^2 - (K^2/4b^2)R^2]F(R) + GF^3(R) = 0 \tag{47}$$

$$\lim_{R \rightarrow 0} F'(R) = 0 \quad \lim_{R \rightarrow \infty} F(R) = 0 \quad F(R) \geq 0. \tag{48a}$$

For $m = \pm 1$, the boundary condition may be written as

$$\lim_{R \rightarrow 0} F(R) = 0 \quad \lim_{R \rightarrow \infty} F(R) = 0 \quad F(R) \geq 0. \tag{48b}$$

The case where $b > 0, z < z_0$ corresponds to the collapse. Given $b < 0, z < z_0$ corresponds to the collapse. Given $b < 0, z > z_0$ in (45) and (46), we obtain a damping solution.

In the first self-similar solution (37) and (38) and in the second one (45) and (46) z_0 is a focusing point, where the field has a singularity. Since two different solutions are obtained here, it is worthwhile to ascertain which of the two solutions is stable and, hence, physically meaningful. To achieve this aim, use was made of computer simulation. It was found out that as $z \rightarrow z_0$ the numerical solution of equation (22) is consistent with the self-similar solution (45) and (46) to high accuracy. Initially, (45) was checked and the constants z_0 and b were determined. Note that a numerical solution was sought for the dimensionless equation and, therefore, to compare with analytical results we set $K = \frac{1}{2}, G = 1, \psi = u(r, z)$ in all the formulae of this section. To confirm the parabolic phase dependence on r , the function $u(r, z)$ was calculated and then the following quantity was evaluated:

$$\delta = \left(\frac{z_0 - z}{r} \right) \left| \frac{\partial}{\partial r} \frac{u(r, z)}{|u(r, z)|} \right|. \tag{49}$$

Here r and z are dimensionless variables (primes are dropped). In figure 4 the results of the computer simulation are presented for $u_0(r) = (\sqrt{8}r^2/m^2) \exp(-r^2/2m^2)$ with $m = 2$. From (46), $\delta = \frac{1}{4}$, which is completely consistent with the computer calculation. For the case under consideration $z_0 = 5.92552, b = 9.63442$. The profile depicted in figure 4 remains practically invariable at $z \geq 5.8$ (the computer test has been carried out up to $z = 5.9255$). To exhaustively check expression (46), we calculated the second quantity

$$\sigma = (z_0 - z) \left| \frac{\partial}{\partial z} \frac{u(r, z)}{|u(r, z)|} \exp\left(\frac{-ir^2}{8(z_0 - z)}\right) \right| \tag{50}$$

which also proved to be independent of r and z at $z \geq 5.8$. It follows from (46) that $\sigma = b\zeta^2 = \text{constant}$. On the other hand, from the computer experimental data and formula (50), it was found that $\sigma \approx 3.64$. Therefore, the parameter ζ^2 determining the function $F(R)$, in accordance with equation (47), has a value of about 0.378 in the case of figure 4.

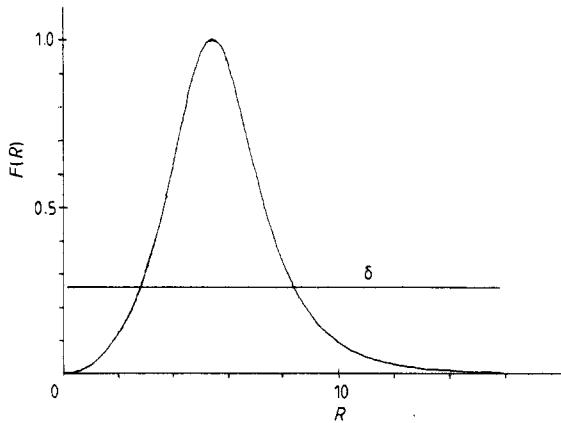


Figure 4. The self-similar structure of the collapsing spiral beam for $m = 2, G = 1, K = \frac{1}{2}$.

In conclusion we note that the self-similar solution for $m = 0$ has been obtained [19]. A more general solution, which is valid for any m , has been found by the above method in [9].

5. Three-dimensional spherically symmetric collapse

As a further development of the collapse theory using the approach presented here, it is noteworthy to consider a three-dimensional case which is claiming the attention of many researchers [20]. For the sake of generality, we consider a three-dimensional collapse described by a Schrödinger-type equation with a non-linearity of the arbitrary power and an explicit dependence on the radius. Thus, consider the following non-linear equation of a more general type:

$$i \frac{\partial}{\partial t} \psi = \frac{1}{r^2} \frac{\partial}{\partial r} \left(r^2 \frac{\partial}{\partial r} \psi \right) + Gr^n |\psi|^s \psi \tag{51}$$

where n and s are arbitrary parameters. We express the complex function $\psi(r, t)$ as

$$\psi(r, t) = A(r, t) \exp(i\phi(r, t)) \tag{52}$$

and then from (51), allowing for (52), we arrive at the system of equations for the real functions $A(r, t)$ and $\phi(r, t)$:

$$A_t = 2\phi_r A_r + [\phi_{rr} + (2/r)\phi_r]A \tag{53}$$

$$(\phi_r^2 - \phi_t)A = A_{rr} + (2/r)A_r + Gr^n A^{s+1}. \tag{54}$$

As in § 4 let the solution for the amplitude be of the form

$$A(r, t) = \alpha(t)Q(\beta(t)r) = \alpha(t)Q(R) \quad R = \beta(t)r. \tag{55}$$

Then equation (53) reduces to

$$\alpha'(t)Q(R) + \alpha(t)\beta'(t)rQ'(R) = 2\phi_r\alpha(t)\beta(t)Q'(R) + [\phi_{rr} + (2/r)\phi_r]\alpha(t)Q(R). \tag{56}$$

Pushing the analogy further, let us seek a particular solution of equation (56) which satisfies the system

$$\alpha'(t) - [\phi_{rr} + (2/r)\phi_r]\alpha(t) = 0 \tag{57}$$

$$\beta'(t) - (2/r)\phi_r\beta(t) = 0. \tag{58}$$

The system represented by (57) and (58) follows from (56) if one equates terms containing $Q(R)$ and $Q'(R)$ in the left- and right-hand sides of (56) separately. From (58) we find

$$(2/r)\phi_r = \gamma(t) \quad \phi(r, t) = \frac{1}{2}\gamma(t)r^2 + \lambda(t) \tag{59}$$

where $\gamma(t)$ and $\lambda(t)$ are some functions of time. Substituting (59) into (57) and (58) we arrive at the equations

$$\alpha'(t) - \frac{3}{2}\gamma(t)\alpha(t) = 0 \tag{60}$$

$$\beta'(t) - \gamma(t)\beta(t) = 0. \tag{61}$$

On the other hand, substituting (55) and (59) into (54) we obtain a basic equation for further analysis:

$$\begin{aligned} & \frac{1}{4}(\gamma^2(t) - \gamma'(t))\beta^{-4}(t)R^2Q(R) - \lambda'(t)\beta^{-2}(t)Q(R) \\ & = Q''(R) + (2/R)Q'(R) + Gr^n\alpha^s(t)\beta^{-2}(t)Q^{s+1}(R). \end{aligned} \tag{62}$$

A self-similar solution is readily seen to exist in the case where the last term in (62) depends only on R . Hence, we find $r^n \alpha^s \beta^{-2} = R^n = r^n \beta^n$ and

$$\alpha(t) = \beta(t)^{(n+2)/s}. \tag{63}$$

Substituting (63) into (60) leads to the equation

$$\beta'(t) - \frac{3}{2} \left(\frac{s}{n+2} \right) \gamma(t) \beta(t) = 0. \tag{64}$$

Comparing (61) with (64) we come to the relationship between indices n and s :

$$s = \frac{2}{3}(n+2) \tag{65}$$

which provides the existence of the self-similar solution. So, on the basis of (63) and (65) we obtain

$$\alpha(t) = \beta^{3/2}(t). \tag{66}$$

Further, we consider two different cases which follow from (62). In the first case we impose the conditions

$$\gamma'(t) - \gamma^2(t) = 0 \tag{67}$$

$$\lambda'(t) + \xi^2 \beta^2(t) = 0. \tag{68}$$

Solving equations (67) and (60) in view of (66), we find

$$\gamma(t) = \frac{1}{t_0 - t} \quad \beta(t) = \frac{a}{t_0 - t} \quad \alpha(t) = \left(\frac{a}{t_0 - t} \right)^{3/2} \tag{69}$$

where t_0 and a are integration constants. Taking account of (69), from (68) we obtain

$$\lambda(t) = \phi_0 - \frac{\xi^2 a^2}{t_0 - t} \quad \phi_0 = \text{constant}. \tag{70}$$

Hence, from (55), (59), (69) and (70) we find the first self-similar solution:

$$A(r, t) = \left(\frac{a}{t_0 - t} \right)^{3/2} Q \left(\frac{ar}{t_0 - t} \right) \tag{71}$$

$$\phi(r, t) = \phi_0 + \frac{r^2 - 4\xi^2 a^2}{4(t_0 - t)} \tag{72}$$

where, in accordance with (62), the function $Q(R)$ satisfies the following equation and boundary conditions:

$$Q''(R) + (2/R)Q'(R) - \xi^2 Q(R) + GR^n Q(R)^{(2n+7)/3} = 0 \tag{73}$$

$$\lim_{R \rightarrow 0} Q'(R) = 0 \quad \lim_{R \rightarrow \infty} Q(R) = 0 \quad Q(R) \geq 0. \tag{74}$$

For $a > 0, t < t_0$ the solutions (71) and (72) describe a collapse, and for $a < 0, t > t_0$ the solution becomes damped. The second self-similar solution is obtained when, according to (62), we require the following conditions to be satisfied:

$$\gamma'(t) - \gamma^2(t) = (1/4a^2)\beta^4(t) \tag{75}$$

$$\lambda'(t) + \xi^2 \beta^2(t) = 0. \tag{76}$$

Solving equations (61), (65) and (75) yields

$$\gamma(t) = \frac{1}{2(t_0 - t)} \quad \beta(t) = \left(\frac{a}{t_0 - t}\right)^{1/2} \quad \alpha(t) = \left(\frac{a}{t_0 - t}\right)^{3/4}. \quad (77)$$

In view of (77), solving (76), we find

$$\lambda(t) = \phi_0 + a\xi^2 \ln \left| \frac{t_0 - t}{a} \right| \quad \phi_0 = \text{constant}. \quad (78)$$

So, taking into account (55), (59), (77) and (78) we obtain the second self-similar solution:

$$A(r, t) = \left(\frac{a}{t_0 - t}\right)^{3/4} Q\left(\left(\frac{a}{t_0 - t}\right)^{1/2} r\right) \quad (79)$$

$$\phi(r, t) = \phi_0 + \frac{r^2}{8(t_0 - t)} + a\xi^2 \ln \left| \frac{t_0 - t}{a} \right|. \quad (80)$$

Here, in accordance with (62), the equation for the function $Q(R)$ and the relevant boundary equations are, respectively,

$$Q''(R) + (2/R)Q'(R) - (\xi^2 - R^2/16a^2)Q(R) + GR^n Q^{(2n+7)/3}(R) = 0 \quad (81)$$

$$\lim_{R \rightarrow 0} Q'(R) = 0 \quad \lim_{R \rightarrow \infty} Q(R) = 0 \quad Q(R) \geq 0. \quad (82)$$

Again, when $a > 0$, $t < t_0$ the solution (79) and (80) describes a collapse, and when $a < 0$, $t > t_0$ the solution has a damped character. Note that for $n = 1$, according to (65), $s = 2$ and the non-linear term of equation (51) has the form $Gr|\psi|^2\psi$. For $n = 0$, we obtain $s = \frac{4}{3}$, and the non-linear term may be written as $G|\psi|^{4/3}\psi$. The same question arises as before (see § 4): which of the two solutions (71), (72) and (79), (80) has a physical meaning? An appropriate analysis and numerical calculation show solution (79)–(82) to be stable.

Thus we have obtained a new class of self-similar solutions which depend on n . In our opinion, among these the case where $n = 1$ seems to be closest to real physical situations which take place, for example, in non-uniform media.

6. Conclusion

The results of the numerical simulations have shown that spiral autoguided beams are periodic along the z axis and solitary in the lateral direction waves. In this respect, they resemble cnoidal and soliton solutions in the theory of exactly integrable non-linear equations. However, it is noteworthy that both these essentially different dependencies on z and r are combined in the spiral autoguide. It is also shown that for $m \neq 0$ the radial distribution of radiation intensity always has a tubular structure. One can strictly prove that the field vanishes on the axis for any $z \geq 0$ and $m \neq 0$ if, at the ($z = 0$) boundary, the field modulus has an annular distribution and $E_0|_{z=0} = 0$.

A qualitative difference of this theory from the theory previously developed [10, 11] is that, because of a spatial phase modulation, there is no diffractive spread here. In particular, it is indicated in § 3 that the integral \tilde{I}_2 determined by (19) becomes

negative for sufficiently large values of z , and consequently the necessary condition is met for the autoguided propagation of spiral beams.

It seems of interest to pay attention to the relation between the results obtained and the theory of self-organising systems. Indeed, analysing the properties of uniform open non-linear systems with time-independent non-equilibrium boundary conditions imposed on them, Glansdorff and Prigogine [21] proved the following statement: stationary states of such systems, which belong to the finite vicinity of the thermodynamic equilibrium state, are asymptotically stable and tend to it monotonically in time. If the distance from equilibrium exceeds some critical value, then the stationary state can become unstable. Thus the Glansdorff and Prigogine theorem is applicable to our case, with the z variable playing the role of time and the pumped power, I_1 , being a bifurcation parameter. When $I_1 < I_c$ the solutions of equation (7) tend monotonically to equilibrium (zero) solutions at $z \rightarrow \infty$. The thermodynamic threshold of self-organisation is achieved when the power exceeds some critical value ($I_1 > I_c$) and the system dynamics in the z variable is determined by the non-linearities available in the system. So, in the case of the cubic non-linearity ($\varepsilon_2 > 0$, $\varepsilon_4 = 0$) the stationary state is unstable at $I_1 > I_c$ and the system changes over to the regime of collapse. When the non-linearity of the fifth order ($\varepsilon_2 > 0$, $\varepsilon_4 < 0$) is considered, the system is shown to change to a new stationary state at $I_1 > I_c$. This is an autoguided propagation with the z periodicity. Thus, at the bifurcation point ($I_1 = I_c$) a dissipative structure arises.

We note that the possibility of the practical use of tubular beams for transmitting information and energy by means of other types of radiation has long been attracting the attention of researchers. In these applications spiral beams have undoubted advantages because of the absence of diffractive divergence.

The spherical collapse is also of great practical interest, offering the possibility of pumping powerful radiation into small volumes. Such three-dimensional collapse can be realised when self-focusing of the convergent spherical wave of radiation takes place in a droplet-like target with a linear dependence of ε_2 on the radial coordinate. The target prepared in such a way ensures the stability of the collapse. In addition, this case is remarkable for the fact that it is analytically tractable. A more detailed description should also include the non-local effect of thermal self-action. Nevertheless, the local approach we have used, which is typical in the self-focusing theory, develops a proper qualitative pattern of the phenomena discussed. Finally, we note that there is a stable solution of equation (4) which describes the two-wave interaction of spiral beams with different topological charges m_1 and m_2 , provided that the polarisation vectors of these waves are orthogonal. In this case, the field intensity radial distribution has a more complicated nature. In particular it may have several maxima.

We hope that the results obtained are sufficiently encouraging to stimulate experimental investigations in this field.

References

- [1] Askaryan G A 1962 *Zh. Eksp. Teor. Fiz.* **42** 1568
- [2] Talanov V I 1964 *Izv. Vuz. Radiofiz.* **14** 479
- [3] Chiao R, Garmire E and Tawnes C 1964 *Phys. Rev. Lett.* **13** 479
- [4] Akhmanov S A, Sukhorukov A P and Khokhlov R V 1967 *Usp. Fiz. Nauk* **93** 19
- [5] Marburger T M 1975 *Prog. Quant. Electron.* **4** 35
- [6] Shen Y R 1975 *Prog. Quant. Electron.* **4** 1
- [7] Kruglov V I and Vlasov R A 1985 *Phys. Lett.* **111A** 401

- [8] Vlasov R A, Volkov V M, Drits V V and Kruglov V I 1987 *Lasery i opticheskaya nelineynost* (Vilnius: Institut Fiziki Akademii Nauk LitSSR) p 250
- [9] Kruglov V I, Volkov V M, Vlasov R A and Drits V V 1987 *Preprint* N490 Institut Fiziki Akademii Nauk BSSR, Minsk
- [10] Askaryan G A 1968 *Zh. Eksp. Teor. Fiz.* **55** 1400
- [11] Askaryan G and Studenov V B 1969 *Zh. Eksp. Teor. Fiz. Pis. Red.* **10** 113
- [12] Paxton A H 1984 *J. Opt. Soc. Am. A* **1** 319
- [13] Vlasov S N, Petrishchev V A and Talanov V I 1970 *Izv. Vuz. Radiofiz.* **12** 1353
- [14] Zakharov V E 1972 *Zh. Eksp. Teor. Fiz.* **62** 1745
- [15] Vlasov S N, Piskunov L V and Talanov V I 1978 *Zh. Eksp. Teor. Fiz.* **75** 1602
- [16] Degtyarev L M and Krylov V I 1977 *Zh. Vych. Mat. Fiz.* **17** 1523
- [17] Zakharov V E, Sobolev V V and Synakh V S 1971 *Zh. Eksp. Teor. Fiz. Pis. Red.* **14** 564
- [18] Frayman G M 1985 *Zh. Eksp. Teor. Fiz.* **88** 390
- [19] Rypdal K, Rasmussen I I and Thomsen K 1985 *Physica* **16D** 339
- [20] Zakharov V E and Kuznetsov E A 1986 *Zh. Eksp. Teor. Fiz.* **91** 1310
- [21] Glansdorff P and Prigogine I 1980 *Thermodynamics: Theory of Structure, Stability and Fluctuations* (New York: Wiley)